Supplementary information to:

Regulating the Electron Density of Dual Transition Metal Sulfides Heterostructures for Highly Efficient Hydrogen Evolution in Alkaline Electrolytes

Miao Yang,[a,b] Yimin Jiang,[a] Shu Liu,[a] Mengjie Zhang, [a] Qifei Guo, [a] Shen Wei, [a] Rongxing He,[*a] Wei Su[*b] and

Ming Li[*]

[a] Key Laboratory of Luminescent and Real-Time Analytical Chemistry (Southwest University), Ministry of Education, College of Chemistry and Chemical Engineering, Southwest University, Chongqing 400715, China
E-mail: herx@swu.edu.cn; liming@swu.edu.cn.
[b] Guangxi Key Laboratory of Natural Polymer Chemistry and Physics, Guangxi Teachers Education University, Nanning 530001, China
E-mail: suwmail@163.com

Experimental Section

Materials and chemicals

NF was purchased from Shenzhen Green and Creative Environmental Science and Technology Co., Ltd. (Shenzhen, China). Hydrochloric acid (HCl), ethanol, carbon disulfide (CS_2), and potassium hydroxide (KOH) were bought from Chongqing Chuandong Chemical Co., Ltd. (Chengdu, China). Ammonium molybdate tetrahydrate ((NH_4)$_6$$Mo_7$$O_{24}$·$4H_2O$) and thiourea ($CH_4N_2S$) were purchased from Aladdin Co,. Ltd. (shanghai, China). Ammonium fluoride (NH_4F) was obtained from Greagent Co,. Ltd. (shanghai, China). All reagents were used as received without any purification. Double distilled water (18.25 MΩ) was used throughout the experiments.

Preparation of NiMoO$_4$·xH$_2$O-NF precursor

NiMoO$_4$·xH$_2$O-NF precursors were first synthesized through hydrothermal treatment with a modification.[1] A piece of commercial NF (2 cm × 3 cm) was washed ultrasonically in 3 M HCl solution, ethanol and DI water alternately for several minutes. In a typical synthetic procedure, 0.01 g NH_4F and 0.155 g (NH_4)$_6$$Mo_7$$O_{24}$·$4H_2O$ were dissolved in 5 mL ultrapure water and 10 mL absolute alcohol under stirring at room temperature to form a uniform solution. Afterward, cleaned NF was placed in the uniform solution. Subsequently, the mixtures with a piece of as-treated NF were transferred into a Teflon-lined stainless steel autoclave (25 mL). Then autoclave was sealed and maintained at 150 °C for 8 h. After reactions

the products were washed with water and ethanol several times, and then dried to obtain $NiMoO_4 \cdot xH_2O$ nanorods arrays on NF as precursor.

Preparation of hierarchical N-NiS/MoS$_2$-NF heterostructures

The $NiMoO_4 \cdot xH_2O$-NF precursor was placed at the center of a tube furnace. Thiourea power was put in another porcelain boat at the upstream side of the precursor. Subsequently, the furnace was increased to 500 °C under flowing inert atmosphere for 2 h. Then the furnace programmatically cooled to room temperature. The as-obtained sample was collected and washed with carbon disulfide and ethanol several times and then dried at 60 °C. The resulting product was denoted as N-NiS/MoS$_2$-NF.

Preparation of NiS$_2$/MoS$_2$-NF

The preparation of NiS$_2$/MoS$_2$-NF 3D electrode are similar to that of the N-NiS/MoS$_2$-NF electrode except for replacing with S power as reactants.

Preparation of Pt/C-NF electrode

10 mg commercial Pt/C (20 wt.%) and 50 μL Nafion solution (5 wt.%) were dispersed in water/ethanol solvent (500 μL distilled water and 450 μL ethanol) by 30 min sonication to form an ink. Then 200 μL catalyst ink was uniformly drop-cast onto the 1x1 cm^2 Ni foam and air-dried at room temperature.

Materials Characterization

X-ray diffraction (XRD) patterns were recorded on a X'Pert Pro MPD , Holland. The morphologies of the materials were characterized using field-emission scanning

electron microscopy (FESEM), JEOL-7800F, Japan. High-resolution transmission electron microscopy (HR-TEM) images were recorded at FEI, TFI220, USA. The surface properties of the samples were investigated using X-ray photoelectron spectroscopy (XPS), Thermo ESCALAB 250XI, USA. The Raman of sample was characterized by Renishaw Invia, England.

Electrochemical Measurements

All electrochemical performance were tested in a typical three-electrode configuration on an electrochemical workstation (CHI 660E, CH Instruments, Inc., Shanghai, China). The as-obtained N-NiS/MoS$_2$-NF was directly used as working electrode. Graphite rod and saturated calomel electrode (SCE) were used as counter and reference electrodes, respectively. All the potentials were calibrated to a reversible hydrogen electrode (RHE) with *iR* compensation. The HER polarization curves were obtained by linear sweep voltammetry (LSV) at a scan rate of 5 mV s^{-1} in 1 M KOH. The electrochemical impedance spectroscopy (EIS) measurements were performed using an AC voltage with 5 mV amplitude in a frequency range from 100 kHz to 10 mHz under 1 M KOH solution. To estimate the electrochemically active surface area (ECSA) of the samples, cyclic voltammetry was applied to probe the electrochemical double-layer capacitance (C_{dl}) at non-faradaic potentials in 1.0 M KOH at different scan rates.

Theoretical basis

Density function theory (DFT) calculations were performed using Dmol[3] code as implemented in the Materials Studios package of Accelrys.[2,3] The electron exchange-correlation potential was conducted by the generalized gradient approximation (GGA) with the Perdew-Burke-Ernzerhof (PBE) functional.[4] The semi-core pseudo potentials (DSPPs) combined with double numerical plus polarization (DNP) basis set were chosen for all of calculations.[5] The convergence tolerances were set to 1.0×10^{-5} hartree for energy change, 2.0×10^{-3} hartree $Å^{-1}$ for maximum force, and 5.0×10^{-3} Å for maximum displacement. The smearing was set to 0.005. The DFT correction (DFT-D) was used to treat the van der Waals interactions by TS method.[6] The Brillouin zone integration was sampled with the $5 \times 5 \times 1$ k-point. The surface was simulated with a single-layer-thick p (3×3) plane slab with $\sim$ 15 Å vacuum.[7] Adsorption energy was calculated by subtracting the energies of gas phase species and clean surface from the total energy of the absorbed system: $E_{ads} = E_{adsorbate/slab} - [E_{adsorbate} + E_{slab}]$. The hydrogen adsorption free energy (ΔG_{H}) was calculated as follows: $\Delta G_H = \Delta E_H + \Delta ZPE - T\Delta S_H$.
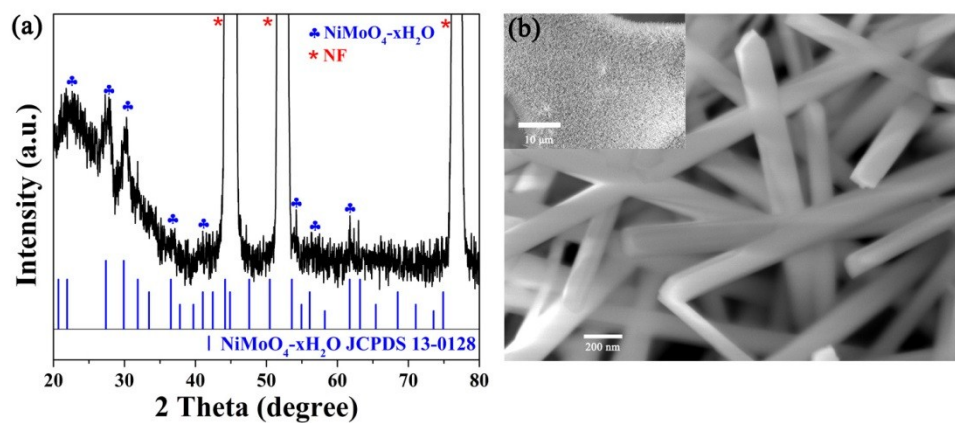
Figure S1. (a) XRD pattern and (b) SEM images of the precursor $NiMoO_4 \cdot xH_2O$-NF.
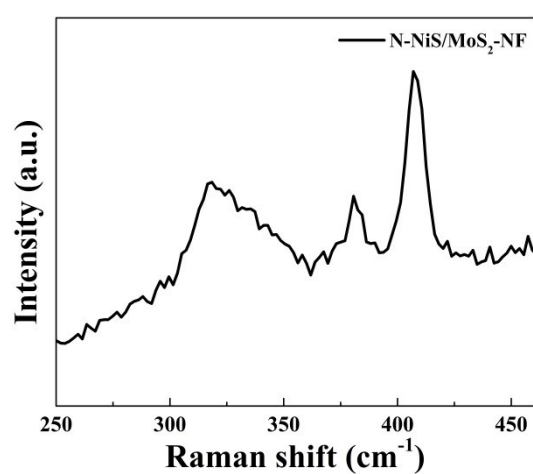
Figure S2. The Raman spectrum of N-NiS/MoS_2 heterostructures.
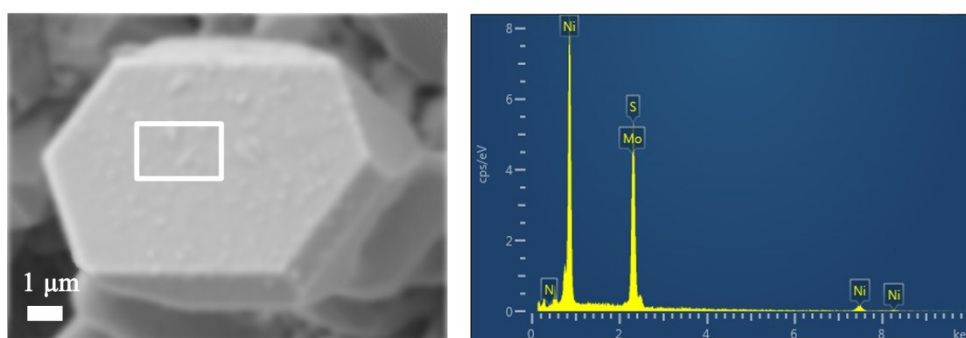
Figure S3. SEM-EDX patterns of N-NiS/MoS_2 heterostructures.
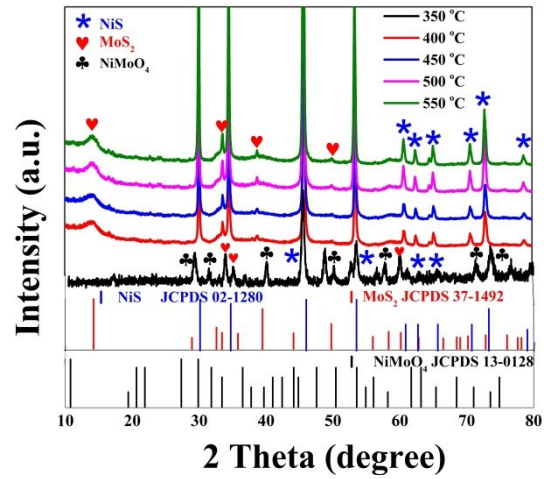
Figure S4. XRD patterns of the samples at different calcination temperature.
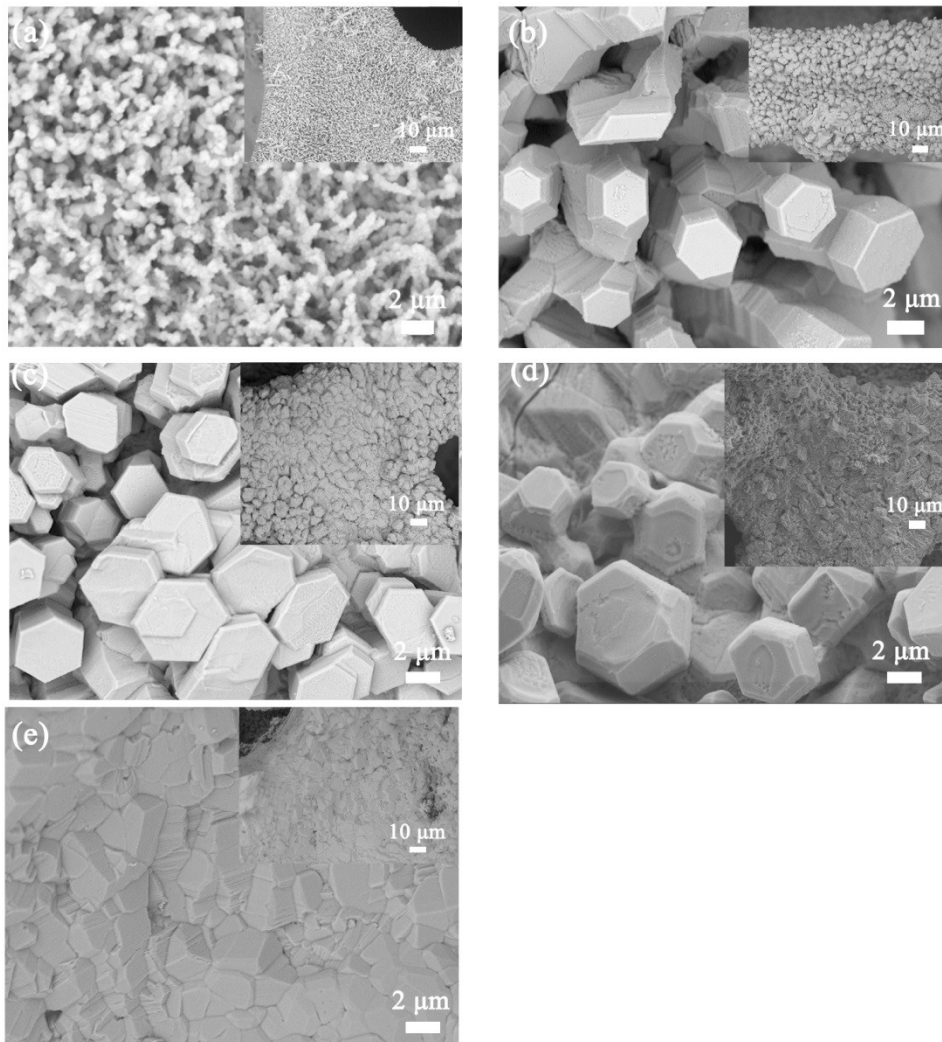
Figure S5. SEM images of the samples at different calcination temperature: (a) 350 °C, (b) 400

°C, (c) 450 °C, (d) 500 °C, and (d) 550 °C.
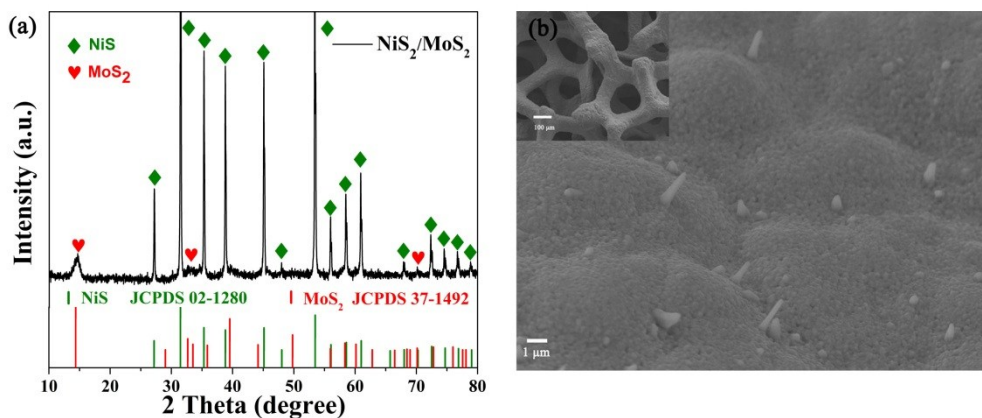
Figure S6. (a) XRD pattern and (b) SEM images of NiS$_2$/MoS$_2$-NF.
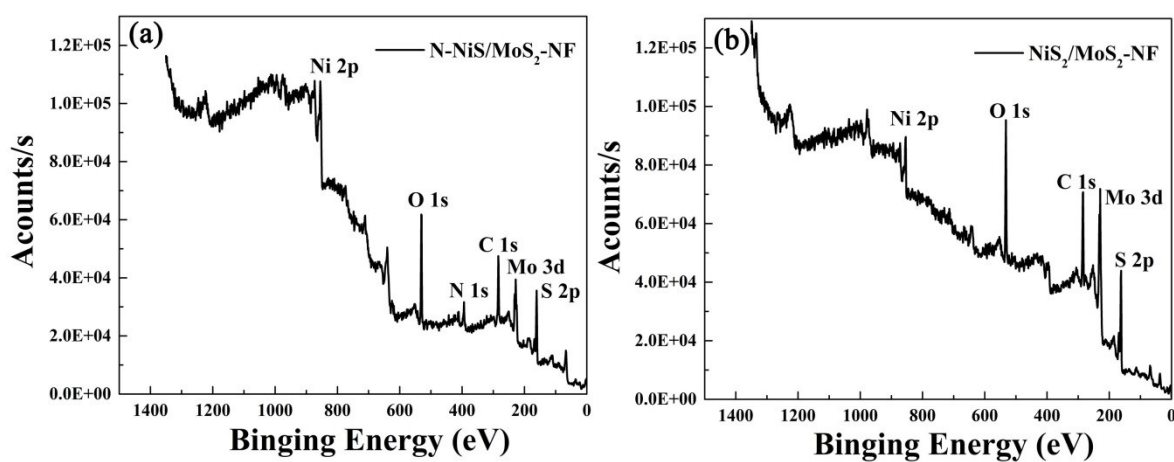
Figure S7. Surface composition and chemical state analyses of (a) N-NiS/MoS$_2$-NF and (b)

NiS$_2$/MoS$_2$-NF. XPS full spectrums.
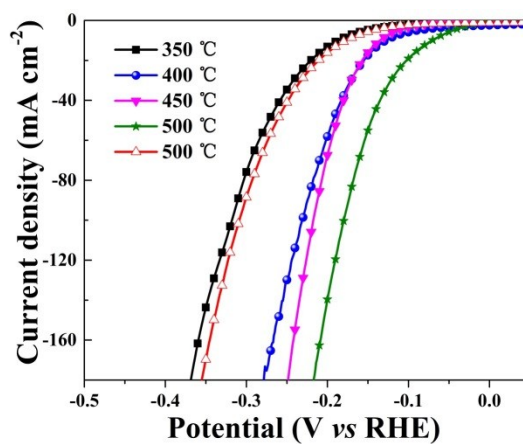
Figure S8. The LSV plots of N-NiS/MoS$_2$-NF prepared at different temperatures.
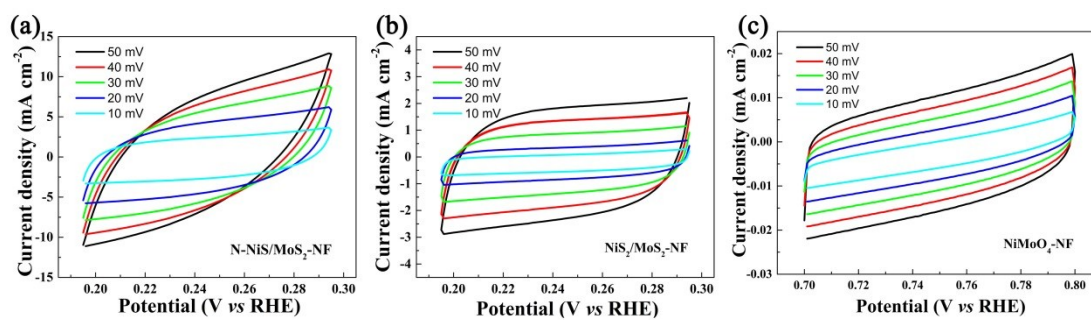
Figure S9. Cyclic voltammograms of (a) N-NiS/MoS$_2$-NF, (b) NiS$_2$/MoS$_2$-NF, and (c) NiMoO$_4$-NF in 1.0 M KOH at various scanning rates (from 5 to 30 mV S^{-1}).
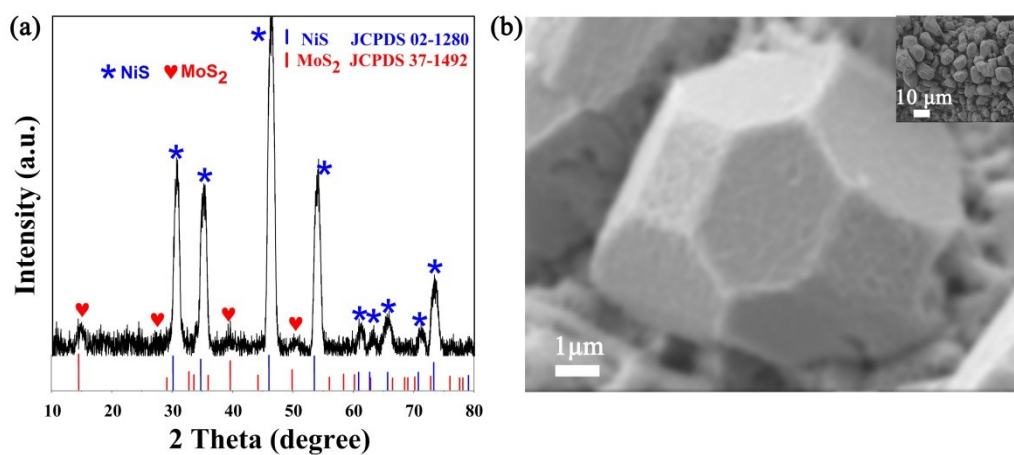
Figure S10. (a) XRD and (b) SEM images of N-NiS/MoS$_2$-NF after stability test.
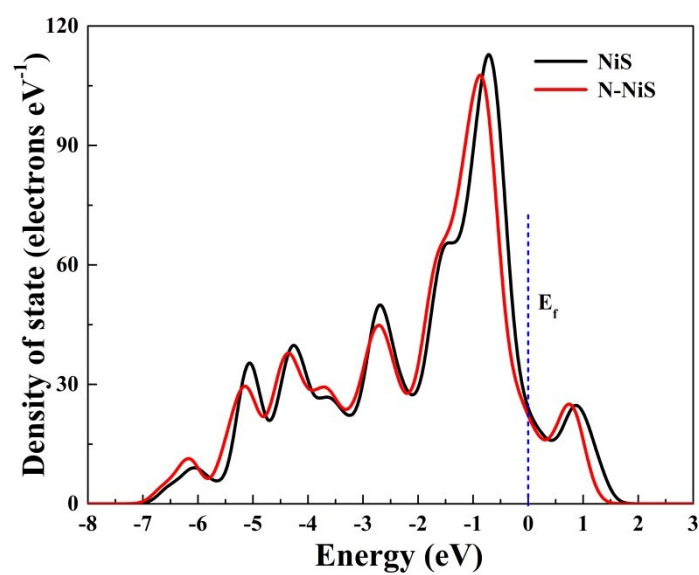
Figure S11. Calculated density of states for NiS and N-NiS. The Fermi Level is set at 0 eV.
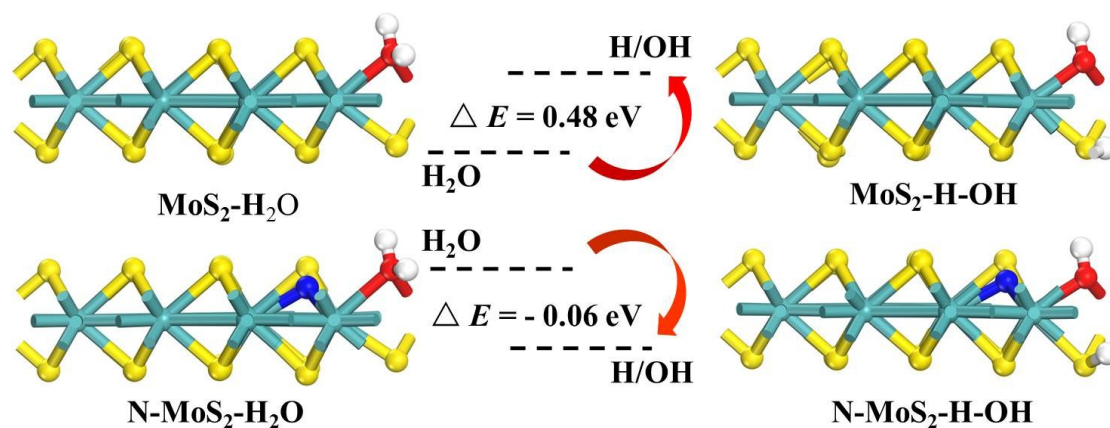
Figure S12. Adsorbed H_2O dissociation configuration on the surfaces of MoS_2 (002) facet and N-MoS_2 (002) facet, as well as corresponding dissociation energies in alkaline solution. Yellow, green, lightt blue, red and white balls represent S, Mo, N, O and H atoms, respectively.
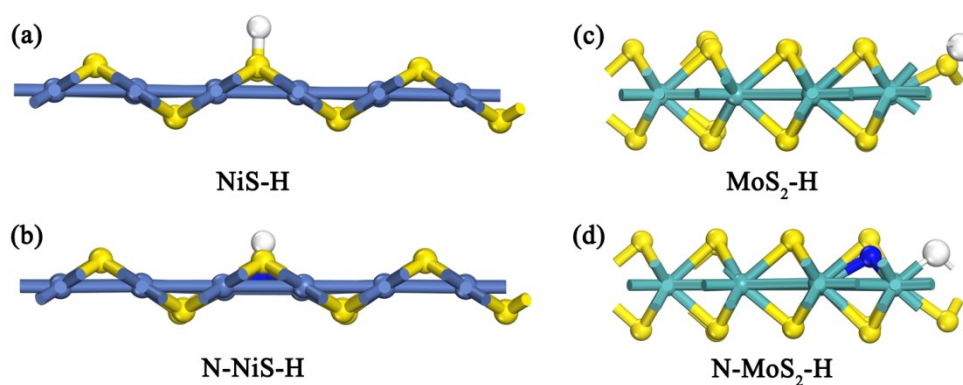
Figure S13. Chemisorption models of H on the surfaces of (a) NiS (100), (b) N-NiS (100), (c) MoS_2 (002), and (d) N-MoS_2 (002). Yellow, dark blue, green, light blue and white balls represent S, Ni, Mo, N and H atoms, respectively.
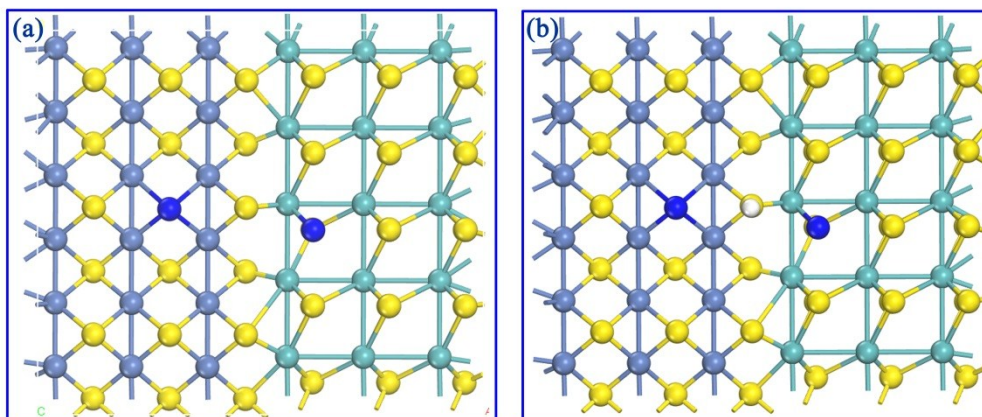
Figure S14. (a) Schematic model of of N-NiS/MoS$_2$; (b) Chemisorption models of H on the surfaces of of N-NiS/MoS$_2$. Yellow, dark blue, green, light blue and white balls represent S, Ni, Mo, N and H atoms, respectively.

Table S1. Comparison of the HER electrocatalytic performance of N-NiS/MoS$_2$ catalysts with reported transition metals sulfide-based electrocatalysts in alkaline condition.

Catalysts	Current Density (j mA cm^{-2})	Overpotential at Corresponding j (mV)	Tafel slope (mV/decade)	Reference
N-CoS$_2$ NW/CC	50	152	58	[7]
MoS$_2$/Ni$_3$S$_2$	10	110	83	[8]
MoS$_2$-Ni$_3$S$_2$	10	98	61	[9]
N-Ni$_3$S$_2$/NF	10	110	-	[10]
NiS$_2$-MoS$_2$	10	204	65	[11]
MoS$_2$/NiS NCs	10	92	113	[12]
NiS/MoS$_2$ nanoflakes	10	117	58	[13]
N-Ni$_3$S$_2$/NF	10	155	113	[14]
Ni-Mo-S nanowire	100	290	103	[15]
MoS$_2$/NiS yolk–shell microspheres	10	244	97	[16]
N-NiS/MoS$_2$-NF	10	71	79	This work

Table S2. Binding energies of H$_2$O on NiS and N-NiS substrates in alkaline solution.

	NiS (eV)	N-NiS (eV)
Binding Energies	-10.47	-10.83

Reference

1. Y. Y. Chen, Y. Zhang, X. Zhang, T. Tang, H. Luo, S. Niu, Z. H. Dai, L. J. Wan and J. S. Hu, *Adv. Mater.*, 2017, **29**, 1703311.

2. B. Delley, *J. Chem. Phys.*, 2000, **113**, 7756-7764.

3. B. Delley, *J. Chem. Phys.*, 1990, **92**, 508-517.

4. J. P. Perdew, K. Burke and M. Ernzerhof, *Phys. Rev. Lett.*, 1996, **77**, 3865-3868.

5. B. Delley, *Phys. Rev. B*, 2002, **66**, 155125.

6. A. Tkatchenko and M. Scheffler, *Phys. Rev. Lett.*, 2009, **102**, 073005.

7. P. Z. Chen, T. P. Zhou, M. L. Chen, Y. Tong, N. Zhang, X. Peng, W. S. Chu, X. J. Wu, C. Z. Wu and Y. Xie, *ACS Catal.*, 2017, **7**, 7405-7411.

8. J. Zhang, T. Wang, D. Pohl, B. Rellinghaus, R. Dong, S. Liu, X. Zhuang and X. Feng, *Angew. Chem. Int. Ed.*, 2016, **55**, 6702-6707.

9. Y. Yang, K. Zhang, H. Lin, X. Li, H. C. Chan, L. Yang and Q. Gao, *ACS Catal.*, 2017, **7**, 2357-2366.

10. P. Chen, T. Zhou, M. Zhang, Y. Tong, C. Zhong, N. Zhang, L. Zhang, C. Wu and Y. Xie, *Adv. Mater.*, 2017, **29,** 1701584.

11. P. Kuang, T. Tong, K. Fan and J. Yu, *ACS Catal.*, 2017, **7,** 6179-6187.

12. Z. J. Zhai, C. Li, L. Zhang, H. C. Wu, L. Zhang, N. Tang, W. Wang and J. L. Gong, *J. Mater. Chem. A*, 2018, **6**, 9833-9838.

13. K. Y. Tao, Y. Gong and J. H. Lin, *Electrochimica Acta*, 2018, **274**, 74-83.

14. T. Y. Kou, T. Smart, B. Yao, I. Chen, D. Thota, Y. Ping and Y. Li, *Adv. Energy Mater.*,

2018, **8**, 1703538.

15.   Z. Ma, H. Meng, M. Wang, B. Tang, J. Li and X. Wang, *ChemElectroChem*, 2018, **5**,

        335-342.

16.   Q. Qin, L. Chen, T. Wei and X. Liu, *Small,* 2018, 1803639.